chemistry proceedings

MDPI

Proceeding Paper

A Refined Model of the CFTR Membrane Transporter as a Tool to Revert Misbehavior

Pedro M. S. Suzano [1,*], Michael González-Durruthy [2], Ricardo J. Ferreira [3], Cátia A. Bonito [4], Margarida D. Amaral [5] and Daniel J. V. A. dos Santos [1,*]

[1] CBIOS—Research Center for Biosciences & Health Technologies, Lusófona University, Campo Grande 376, 1749-024 Lisboa, Portugal
[2] INL—International Iberian Nanotechnology Laboratory, Avenida Mestre José Veiga s/n, 4715-330 Braga, Portugal; gonzalezdurruthy.furg@gmail.com
[3] Red Glead Discovery, Medicon Village, Building 403, Scheeletorget 1, 223 81 Lund, Sweden; ricardo.ferreira@redglead.com
[4] Medicinal Chemistry, Research and Early Development, Cardiovascular, Renal and Metabolism (CVRM), BioPharmaceutical R&D, AstraZeneca, Gothenburg, Sweden; catia.bonito.ferreira@gmail.com
[5] BioISI—Biosystems & Integrative Sciences Institute, Faculty of Sciences, University of Lisboa, Campo Grande, C8, 1749-016 Lisboa, Portugal; msamaral@ciencias.ulisboa.pt
* Correspondence: p7857@ulusofona.pt (P.M.S.S.); daniel.dos.santos@ulusofona.pt (D.J.V.A.d.S.)

Abstract: ABC proteins are large transmembrane efflux pumps that export substrates against the concentration gradient through ATP hydrolysis. Due to their efflux capabilities, they are crucial in drug metabolism. Point mutations in ABC proteins can lead to many forms of illness by causing protein misfolding and misbehavior. CFTR, or ABCC7, is a member of this transporter family, which, when mutated, can lead to cystic fibrosis, the most common life-shortening rare disease. Herewith, we report on a refined and functional model of CFTR using in silico methods, aiming at further understanding anion permeation and the impact of different mutations on the gating mechanism to bring light on ways to reverse mutations' effects.

Keywords: cystic fibrosis; molecular modeling; ABC Efflux Transporters; molecular dynamics

Citation: Suzano, P.M.S.; González-Durruthy, M.; Ferreira, R.J.; Bonito, C.A.; Amaral, M.D.; Santos, D.J.V.A.D. A Refined Model of the CFTR Membrane Transporter as a Tool to Revert Misbehavior. *Chem. Proc.* **2024**, *6*, x. https://doi.org/10.3390/xxxxx

Academic Editor(s): Name

Published: 15 November 2024

1. Introduction

Cystic fibrosis (CF) is a genetic disorder mostly found in European populations, specifically those from northern Europe. It is estimated to affect over 100,000 people worldwide, causing progressive damage to the lungs and pancreas [1]. Due to a very low life expectancy associated with this condition, CF has been considered the most common deadly genetic disorder of children in these populations. However, advancements in CF therapeutics from recent decades have enabled those affected to live, on average, close to 50 years [2].

The gene responsible for CF and coding for the cystic fibrosis transmembrane conductance regulator (CFTR) was successfully cloned in 1989 by Riordan and coworkers [3]. Since then, several therapies have been developed to improve the life expectancy and quality of these patients by targeting the genetic defect. This proved to be quite complex, as today, more than 2000 mutations in the CFTR gene have been found to cause CF. Despite this variety, around 80% of CF cases present a deletion of residue F508, making it the most problematic and common mutation [4]. Thus, targeting this variant has been the main goal of CF research in the past few decades.

The discovered CFTR mutations were grouped into 6 main classes, regarding their effects in cellular phenotypes. Class I is related with a lack of expression, class II is characterized by folding disabilities, and class III is associated with gating defects. Class IV is marked by conductance defects, while class V mutations lead to a significantly lower quantity in CFTR proteins and class VI mutations produce a very low amount of surface proteins. The F508del mutation is a class II mutation, meaning the CFTR protein fails to fold properly and is flagged for proteosomal degradation [4–6]. Hence, designing therapies for this phenotype can be achieved by focusing on rescuing the CFTR protein by correcting protein folding and increasing its activity.

To date, the most successful therapy option in the market for this deletion is a combination of three modulators named Trikafta. Trikafta is the FDA approved therapy combining the effects of two folding correctors (VX-661 or tezacaftor and VX-445 or elexacaftor), necessary to rescue the defective protein, and a gating potentiator (VX-770 or Ivacaftor) which boosts gating function [4,5]. Despite the overall success and applicability of this form of therapy, the full mechanism of action of some of these compounds is not yet fully understood and insights into many of the rare mutant forms are scarce. Hence, a functional model of the CFTR protein would be valuable for understanding structural effects and details of these interaction changes.

CFTR, also known as ABCC7, belongs to the ABC (ATP-Binding Cassette) superfamily of proteins. It differs from most other proteins in this family, as many are known membrane transporter proteins while CFTR is an ion channel, using ATP binding and hydrolysis in anion translocation [7]. Still, CFTR shares structural similarities with many proteins in this family: it features two transmembrane domains (TMDs) that cross the membrane facilitating substrate crossing and two nucleotide binding domains (NBDs), facing the cytoplasm, that are responsible for ATP recognition, binding and hydrolysis [8]. However, the architecture of the CFTR protein differs from other ABC transporters in the regulatory domain (R domain) [7,9].

Over the years, electrophysiological studies have demonstrated the importance of the R domain in the substrate transport process. This domain needs to undergo phosphorylation by protein kinase A (PKA) to allow the shift between the closed and open channel states [7,9,10]. Despite the importance of this domain, and the increasing number of available crystallographic structures, a resolved structure of the protein including the R domain does not exist, as of today. It is our opinion that a functional and refined model of the CFTR protein would be quite important to fully understand the mechanistic aspects of ion translocation, effects of modulators and correctors, and effects of point mutations in the CFTR protein.

Chen and coworkers postulate that some regions of the CFTR R domain are likely helical [9]. However, due to being mostly unstructured and quite long, a full refined model of this domain does not yet exist. To circumvent this, we researched functional R domain deletions. We found that deleting aminoacids 708–835 generated a CFTR channel that was constitutively active [11]. Thus, by deleting this portion of the R domain, we generated an active channel that can be useful to study CFTR mechanics and the effects of aminoacid mutations and deletions.

2. Methods

The CFTR atomistic model was built starting with the cryo-electron microscopy (cryo-EM) 6O2P deposited in the protein data bank (PDB) [12]. Although this structure describes the interaction with the ivacaftor potentiator, several segments could not be atomistically resolved although it is, so far, the most complete resolved sequence.

To obtain a complete and functional atomistic model, we followed a protocol already successfully used to build the atomistic structures of Pgp [13] and BCRP [14]. Specially in the case of Pgp, the importance of including missing sequences that are relevant for function and/or structural stability was quite clear [13,15].

The third chain of PDB structure 6O2P containing co-crystallized molecules/ions like ATP, was removed and the protein was saved in a PDB file to be used as the starting point for model building. The second protein chain, containing a short sequence for which the side chains were not resolved, was kept to be used in the modeling. Both ATP and the corresponding magnesium ions were also saved on another file to be later included in the simulations. All other molecules were not used.

The missing segments were built using the Molecular Operating Environment (MOE v2019.01 [16]). Three short missing sequences exist between amino acids 410–436 and 1174–1201 (loops connecting a TMD with the NBD that follows in the sequence), and 890–899 (extracellular loop 4, uniting helices 7 and 8). The R domain (638–844) that needs to be phosphorylated to allow the channel to open, is also mostly unmapped. However, for 17 amino acids (half organized as helix) although their position is known, the side chains are not resolved and, therefore, their relative position in the sequence is unknown.

For small missing sequences, a search was made in MOE using the Loop/Linker Modeler module and the best scored loop was used. However, since the R domain is too large to be correctly modeled and positioned, we used a different approach. Experimentally, it was demonstrated that the R domain could be shortened while keeping the CFTR function [11].

To model the end part of the R domain sequence until Thr844, the "predictprotein" server was used [17]. The mapped helix starting at Thr845 to Ile853 was included in the sequence uploaded to the server to match this helix sequence with the prediction and to assign the rest of the sequence. MOE's Protein Builder was used to build this sequence as predicted by the server. For the remaining R domain sequence, the MOE's Protein Builder was also used by choosing an extended geometry conformation for each added amino acid, always followed by a simple energy minimization using default parameters and linking the last added amino acid to the next known amino acid position.

All the added protein sequences were assembled in a PDB file. To correctly maintain the physiological function of CFTR, the experimentally known amino acids that need to be phosphorylated, were phosphorylated using the CHARMM36 force field used throughout. The experimentally reported phosphorylated amino acids kept in the CFTR model where Ser422 (in NBD1), and Ser660, Ser670, Ser700, in the R domain [18]. When needed, the charmm-gui web server was used to convert MOE's PDB to the corresponding CHARMM36 atom types. To allow the newly modeled sequences to better adjust to their environment, the assembled CFTR protein was solvated and neutralized to be used in a *NVT* simulated annealing from 303 to 323 K using 10 points for a total simulation time of 10 ns, while keeping all protein position restrained but the added sequences. Except when otherwise stated, all simulations were executed in GROMACS (v2019.3).

A POPC bilayer containing 512 lipids and 20,480 water molecules was assembled from a previously used smaller POPC patch. This patch in water was equilibrated at *NpT* (1 bar, 303K), using parameters like those used for the fully assembled CFTR system and described below. The g_membed GROMACS (v4.6.2) program was used to embed the CFTR on the POPC bilayer patch and the position of the membrane relative to CFTR was defined using information obtained from the OPM database [19]. The number of lipids with the CFTR embedded in the bilayer was reduced to 468.

The system containing the CFTR protein embedded in the POPC patch and the ATP and magnesium ions previously saved from the 6O2P PDB structure were solvated. Other

ions were also added to neutralize the system and the final system contains 468 lipids, 65,170 waters, 24 chlorine ions, 11 sodium ions, 2 ATP and 2 magnesium ions in a box of size about x = 125, y = 131 and z = 166 Å. An energy minimization using the steepest descent algorithm and default converging parameters were used and an *NVT* simulation was performed for just 50 ps to complete the fast adjustment of atoms and to let pressure stabilize.

A run at *NpT* is conducted for 200 ns to equilibrate the system followed by 3 replicates starting with different velocities sampled from the respective Maxwell-Boltzmann velocity distribution in accordance to a temperature of 303 K to collect statistics for production analysis. In all simulations, periodic boundary conditions (PBC) were applied in all three axes. For *NVT*, the Nosé-Hoover thermostat [20,21] was used with a coupling constant of 0.2 ps. For *NpT* simulations, a Parrinello-Rahman barostat [22–24] with a 5 ps semiisotropic (x and y) coupling and a system compressibility of 4.5×10^{-5} bar^{-1} was used. The time-step was 2fs, and data was collected periodically to trajectory and energy files.

The Particle Mesh Ewald (PME) summation method for the electrostatic interactions used cubic interpolation, with an identical cutoff radius for electrostatic and short-range Lennard-Jones interactions (12 Å), was employed. The SETTLE (for water molecules) o LINCS algorithms were used to constrain bond lengths with hydrogen atoms.

3. Results and Discussion

After the system was built and calibrated, it became imperative to analyze and test the overall system health, guaranteeing no significant alterations resulted from the deletion. In Figure 1, the system's structural fluctuations during a 500 ns production run can be observed. The root mean square deviation (RMSD) of alpha carbons belonging to the protein main chain was used to study the system stability. The three modeled missing regions present significantly higher RMSD values than the rest of the protein, suggesting much higher mobility and the underlying reason for the lack of structural information in the experimental structures deposited in the PDB. The R domain, due to having been spliced in our model, tends to stick to the body of the protein and presents significantly lower movement. Our results show that this shorter domain model could probably be determined by cryo-EM, shedding light on a shorter but functional R domain.

The TMDs and NBDs are quite stable along the simulations and the contributions of the added protein sequences has a smaller impact in the global changes of the protein.

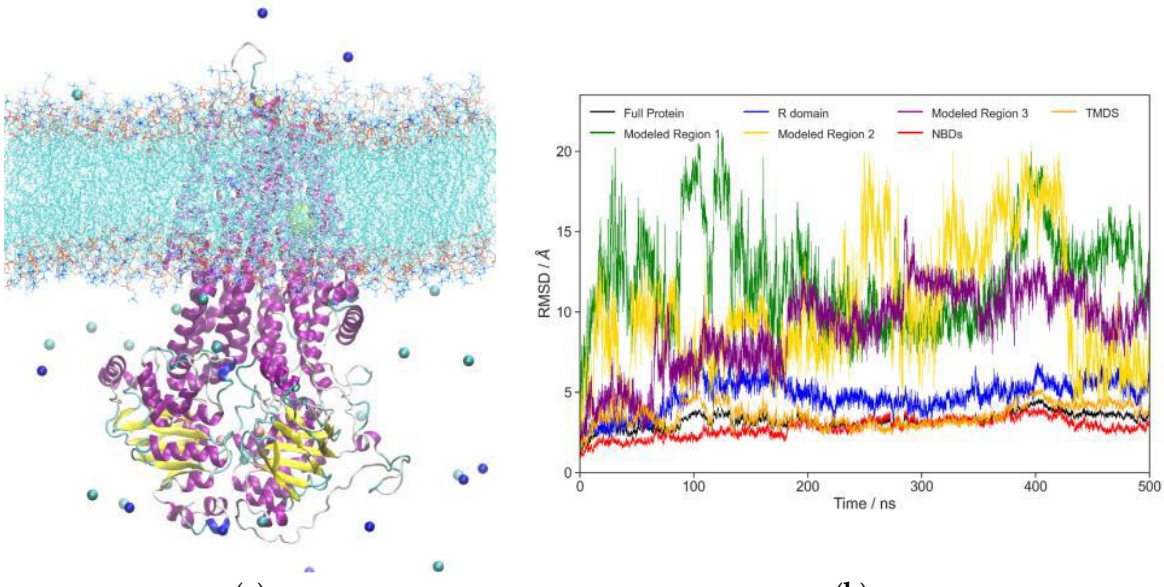

(**a**) (**b**)

Figure 1. (**a**)—Representation of the CFTR model. Ions are represented in light and dark blue spheres. Protein helices are in purple and beta sheets are in yellow. Lipid bilayer is in light blue

sticks with orange phosphates and, for clarity, waters were not depicted. (**b**)—Root mean square deviations over a 500 ns production run. Total modeled protein RMSD in black, TMDs in orange and NBDs in red. Modeled regions 1 (amino acids 410–436), 2 (890–899) and 3 (1174–1201) are in green, yellow and purple, respectively. R domain RMSD is represented in blue.

To further understand protein stability, a root mean square fluctuation (RMSF) analysis was performed on the modeled CFTR, measuring the average deviation of atomic positions from their mean positions over time. In Figure 2, the specific modeled sequences can be compared to the fluctuation of all other residues. Herein, it is possible to verify that the most mobile regions are indeed the four regions missing in the original structure.

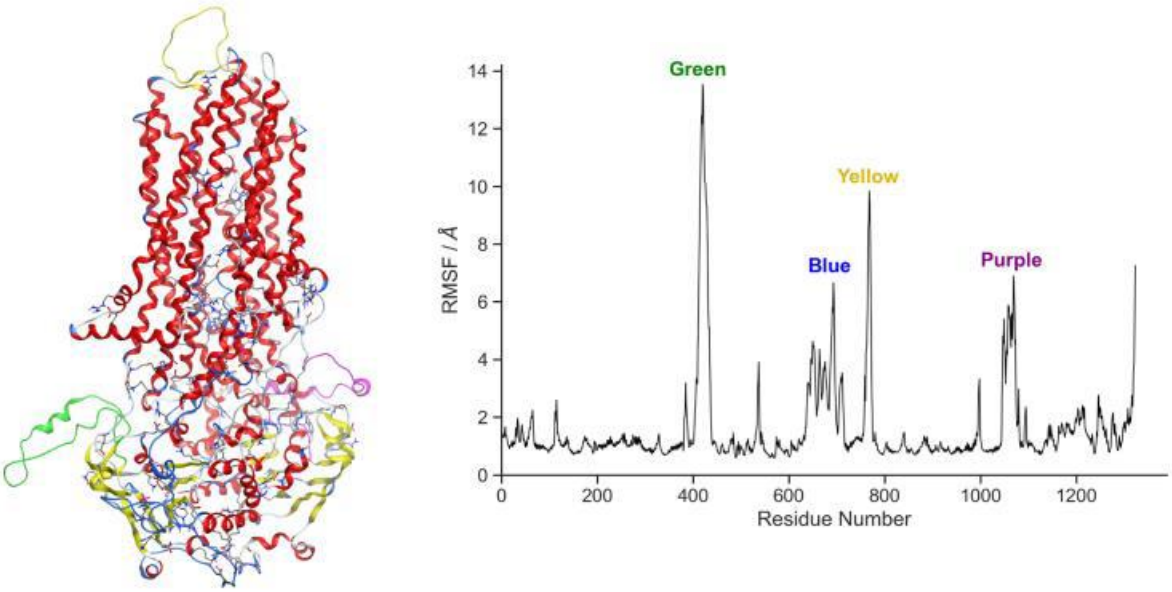

(**a**) (**b**)

Figure 2. (**a**)—CFTR represented in cartoon. Modeled sequence 1 (amino acids 410–436) is in green, the R domain is in blue and modeled sequences 2 (890–899) and 3 (1174–1201) are in yellow (loop on the top of the structure) and pink, respectively. (**b**)—Root mean square fluctuations per protein residue. Higher peaks mean larger average deviation from the mean atomic positions.

As an ion gate, CFTR needs to be open to both ions and waters. Hence, to check our system for functionality, we analyzed the pore in the center of the protein. In Figure 3, the transmembrane region of the protein (where most waters accumulate, and ions diffuse) is visible. Aside from the standard water flow that was observed, we found that some chlorine ions could move in and out of the protein pore (maximum of two; no sodium ions were ever found inside the channel) but never transpose the bilayer to the what corresponds to the extracellular space (there is no ion gradient and, due to the PBC, both sides of the bilayer are in indirect contact trough the simulation box *xy* wall). Moreover, waters seem to stack outside the main pore, near the proposed binding site for Ivacaftor. This find is very interesting and requires further investigation, as it could lead to a greater understanding of one of the most powerful CFTR potentiator compounds with specific characteristics to bind in a quite peculiar environment: hydrophobic helices of the protein, matching the hydrophobic slab of the bilayer although in a pocket that attracts water molecules.

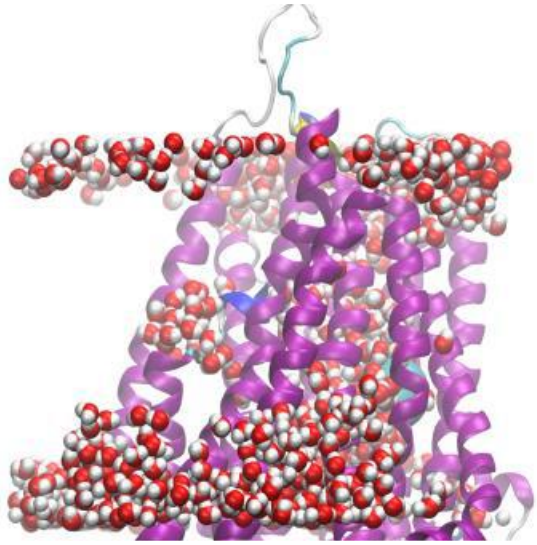

Figure 3. Cartoon representation of the CFTR ion channel with waters crossing the pore. Waters are represented as red and white spheres and protein TMD in purple. Waters inside the bilayer and outside the pore can be seen on the left side. A chlorine ion inside the channel is depicted as a large cyan ball.

4. Conclusions

Herein, a functional CFTR refined structure was obtained (DeltaR(708-835)-CFTR) that correlates to the behavior of the WT CFTR with one or two chlorine ions moving spontaneously to and inside the channel. In fact, in a following simulation already performed of a mutated model (G85E; not yet published), the chlorine ion is very quickly evicted from the channel and, in opposition to the present sliced WT model, no other chlorine ion ever returns to the channel. This needs further analysis and evaluation, but could be the basis for understanding the mechanism of cystic fibrosis condition due to this mutation and could be used to further simulate other CFTR mutated structures. Through this work, the chlorine ion channel exit could be determined and the binding site of the potentiators and their mechanism of action can be clarified in the future.

Although several new experimental structures became available, there are few computational models so far. One model by Tieleman and co-workers used the incomplete structure of the zebrafish to study the structural role of TM8 [25]. Another zebrafish CFTR model by Hegedüs and co-workers [26] used metadynamics simulations to reveal two possible exits on the channel and, more recently, Pomès and co-workers [27] used strong hyperpolarizing electric field to study the translocation of chlorine ions. However, although these simulations used models corresponding to a phosphorylated state, none used an atomistic description containing phosphorylated residues which can impact the behavior of the models and, like the herein described model, only the latter used the human CFTR sequence.

Author Contributions: All authors but P.M.S.S. contributed to the conceptualization of the experiments and methodology. All authors participated in writing and/or revising the manuscript; Simulations were performed by D.J.V.A.d.S. and M.G.-D.; analysis of the simulations by P.M.S.S. and D.J.V.A.d.S.; resources provided by D.J.V.A.d.S. and M.D.A. All authors have read and agreed to the published version of the manuscript.

Funding: This work received financial support from the European Union (FEDER funds POCI/01/0145/FEDER/007265) and National Funds (FCT/MEC, Fundação para a Ciência e Tecnologia and Ministério da Educação e Ciência) under the Partnership Agreement

PT2020UID/QUI/50006/2013 and H2020 PTDC/MED-QUI/28800/2017. Cátia C. Bonito acknowledges the PhD grant SFRH/BD/130750/2017 from FCT.

Institutional Review Board Statement:

Informed Consent Statement:

Data Availability Statement: A final confirmation of the MD refined CFTR structure and all files needed to perform GROMACS simulations are available for download at our website (http://chemistrybits.com).

Conflicts of Interest:

References

1. Kim, C.; Higgins, M.; Liu, L.; Volkova, N.; Zolin, A.; Naehrlich, L.; Andreas, P.; Elise, L.; Duška, T.-D.; Pavel, D.; et al. Effectiveness of Lumacaftor/Ivacaftor Initiation in Children with Cystic Fibrosis Aged 2 through 5 Years on Disease Progression: Interim Results from an Ongoing Registry- Based Study. *J. Cyst. Fibros.* **2024**, *23*, 436–442. https://doi.org/10.1016/j.jcf.2024.02.004.
2. Scotet, V.; L'Hostis, C.; Férec, C. The Changing Epidemiology of Cystic Fibrosis: Incidence, Survival and Impact of the CFTR Gene Discovery. *Genes* **2020**, *11*, 589. https://doi.org/10.3390/genes11060589.
3. Riordan, J.R.; Rommens, J.M.; Kerem, B.-S.; Alon, N.; Rozmahel, R.; Grzelczak, Z.; Zielenski, J.; Lok, S.; Plavsic, N.; Chou, J.-L.; et al. Identification of the Cystic Fibrosis Gene: Cloning and Characterization of Complementary DNA. *Science* **1989**, *245*, 1066–1073.
4. Veit, G.; Roldan, A.; Hancock, M.A.; Da Fonte, D.F.; Xu, H.; Hussein, M.; Frenkiel, S.; Matouk, E.; Velkov, T.; Lukacs, G.L. Allosteric Folding Correction of F508del and Rare CFTR Mutants by Elexacaftor-Tezacaftor-Ivacaftor (Trikafta) Combination. *JCI Insight* **2020**, *5*, e139983. https://doi.org/10.1172/jci.insight.139983.
5. Dastoor, P.; Muiler, C.; Garrison, A.; Egan, M.; Carlos Dos Reis, D.; Santos, A.; Ameen, N.A. Localization and Function of Humanized F508del-CFTR in Mouse Intestine Following Activation of Serum Glucocorticoid Kinase 1 and Trikafta. *Eur. J. Pharmacol.* **2024**, *978*, 176771. https://doi.org/10.1016/j.ejphar.2024.176771.
6. Yeh, J.; Yu, Y.; Hwang, T. Structural Mechanisms for Defective CFTR Gating Caused by the Q1412X Mutation, a Severe Class VI Pathogenic Mutation in Cystic Fibrosis. *J. Physiol.* **2019**, *597*, 543–560. https://doi.org/10.1113/JP277042.
7. Liu, F.; Zhang, Z.; Csanády, L.; Gadsby, D.C.; Chen, J. Molecular Structure of the Human CFTR Ion Channel. *Cell* **2017**, *169*, 85–95.e8. https://doi.org/10.1016/j.cell.2017.02.024.
8. Alam, A.; Locher, K.P. Structure and Mechanism of Human ABC Transporters. *Annu. Rev. Biophys.* **2023**, *52*, 275–300. https://doi.org/10.1146/annurev-biophys-111622-091232.
9. Zhang, Z.; Liu, F.; Chen, J. Molecular Structure of the ATP-Bound, Phosphorylated Human CFTR. *Proc. Natl. Acad. Sci. USA* **2018**, *115*, 12757–12762. https://doi.org/10.1073/pnas.1815287115.
10. Levring, J.; Terry, D.S.; Kilic, Z.; Fitzgerald, G.; Blanchard, S.C.; Chen, J. CFTR Function, Pathology and Pharmacology at Single-Molecule Resolution. *Nature* **2023**, *616*, 606–614. https://doi.org/10.1038/s41586-023-05854-7.
11. Ostedgaard, L.S.; Baldursson, O.; Welsh, M.J. Regulation of the Cystic Fibrosis Transmembrane Conductance Regulator Cl− Channel by Its R Domain. *J. Biol. Chem.* **2001**, *276*, 7689–7692. https://doi.org/10.1074/jbc.R100001200.
12. Liu, F.; Zhang, Z.; Levit, A.; Levring, J.; Touhara, K.K.; Shoichet, B.K.; Chen, J. Structural Identification of a Hotspot on CFTR for Potentiation. *Science* **2019**, *364*, 1184–1188. https://doi.org/10.1126/science.aaw7611.
13. Ferreira, R.J.; Ferreira, M.-J.U.; dos Santos, D.J.V.A. Insights on P-Glycoprotein's Efflux Mechanism Obtained by Molecular Dynamics Simulations. *J. Chem. Theory Comput.* **2012**, *8*, 1853–1864. https://doi.org/10.1021/ct300083m.
14. Ferreira, R.J.; Bonito, C.A.; Cordeiro, M.N.D.S.; Ferreira, M.-J.U.; dos Santos, D.J.V.A. Structure-Function Relationships in ABCG2: Insights from Molecular Dynamics Simulations and Molecular Docking Studies. *Sci Rep* **2017**, *7*, 15534. https://doi.org/10.1038/s41598-017-15452-z.
15. Ferreira, R.J.; Ferreira, M.-J.U.; dos Santos, D.J.V.A. Assessing the Stabilization of P-Glycoprotein's Nucleotide-Binding Domains by the Linker, Using Molecular Dynamics. *Mol. Inform.* **2013**, *32*, 529–540. https://doi.org/10.1002/minf.201200175.
16. Molecular Operating Environment (MOE); 2009.10 Chemical Computing Group ULC. 910-1010 Sherbrooke St. W., Montreal, QC H3A 2R7, 2009.
17. Bernhofer, M.; Dallago, C.; Karl, T.; Satagopam, V.; Heinzinger, M.; Littmann, M.; Olenyi, T.; Qiu, J.; Schütze, K.; Yachdav, G.; et al. PredictProtein—Predicting Protein Structure and Function for 29 Years. *Nucleic Acids Res.* **2021**, *49*, W535–W540. https://doi.org/10.1093/nar/gkab354.
18. Bozoky, Z.; Krzeminski, M.; Chong, P.A.; Forman-Kay, J.D. Structural Changes of CFTR R Region upon Phosphorylation: A Plastic Platform for Intramolecular and Intermolecular Interactions. *FEBS J.* **2013**, *280*, 4407–4416. https://doi.org/10.1111/febs.12422.
19. Lomize, M.A.; Lomize, A.L.; Pogozheva, I.D.; Mosberg, H.I. OPM: Orientations of Proteins in Membranes Database. *Bioinformatics* **2006**, *22*, 623–625. https://doi.org/10.1093/bioinformatics/btk023.

20. Nosé, S. A Molecular Dynamics Method for Simulations in the Canonical Ensemble. *Mol. Phys.* **1984**, *52*, 255–268. https://doi.org/10.1080/00268978400101201.
21. Hoover, W.G. Canonical Dynamics: Equilibrium Phase-Space Distributions. *Phys. Rev. A* **1985**, *31*, 1695–1697. https://doi.org/10.1103/PhysRevA.31.1695.
22. Parrinello, M.; Rahman, A. Crystal Structure and Pair Potentials: A Molecular-Dynamics Study. *Phys. Rev. Lett.* **1980**, *45*, 1196–1199. https://doi.org/10.1103/PhysRevLett.45.1196.
23. Parrinello, M.; Rahman, A. Polymorphic Transitions in Single Crystals: A New Molecular Dynamics Method. *J. Appl. Phys.* **1981**, *52*, 7182–7190. https://doi.org/10.1063/1.328693.
24. Parrinello, M.; Rahman, A. Strain Fluctuations and Elastic Constants. *J. Chem. Phys.* **1982**, *76*, 2662–2666. https://doi.org/10.1063/1.443248.
25. Corradi, V.; Gu, R.-X.; Vergani, P.; Tieleman, D.P. Structure of Transmembrane Helix 8 and Possible Membrane Defects in CFTR. *Biophys. J.* **2018**, *114*, 1751–1754. https://doi.org/10.1016/j.bpj.2018.03.003.
26. Farkas, B.; Tordai, H.; Padányi, R.; Tordai, A.; Gera, J.; Paragi, G.; Hegedűs, T. Discovering the Chloride Pathway in the CFTR Channel. *Cell. Mol. Life Sci.* **2020**, *77*, 765–778. https://doi.org/10.1007/s00018-019-03211-4.
27. Zeng, Z.W.; Linsdell, P.; Pomès, R. Molecular Dynamics Study of Cl− Permeation through Cystic Fibrosis Transmembrane Conductance Regulator (CFTR). *Cell Mol Life Sci* **2023**, *80*, 51. https://doi.org/10.1007/s00018-022-04621-7.